

Functionalization of ceramic fibers by metallic sputter coating

Qufu Wei, Dongfeng Shao, Bingyao Deng,
Qiuxiang Xu

© FSCT and OCCA 2009

Abstract Ceramic fibers were functionalized by the sputter coating of copper in this study. The surface and interface structures of the functionalized ceramic fibers were investigated by atomic force microscopy (AFM) and environmental scanning electron microscopy (ESEM). The observations by AFM revealed the formation of nanoclusters on the fiber surface. The coated layer of the sputtered copper was also confirmed by the ESEM examination, equipped with an energy-dispersive X-ray analysis. It was also found that the electrical resistance of the ceramic fibers decreased with increased coating thickness. The interfacial bonding between fibrous substrate and sputter-coated copper was investigated and discussed by peel-off tests in this study. The mechanism of the interfacial adhesion between copper and fiber substrate was also discussed.

Keywords Ceramic fibers, Sputter coating, Surface, AFM, ESEM, Metal

Introduction

A family of oxide fibers—ceramic oxide fiber—has been developed specifically for the reinforcement of metal and ceramic matrix composites.¹ Ceramic fibers are produced by chemical vapor deposition (CVD), melt drawing, spinning, and extrusion. The main advantage of ceramic fibers is their high strength and modulus. Ceramic fiber is a type of new heat insulation refractory and inorganic material. Ceramic fibers have

been manufactured in various forms for a wide range of heat insulation and composite applications.

Ceramic fibers have also been used as the carrier matrix of the catalyst to support copper–zinc oxide catalyst powders.² Catalyst particles supported on the ceramic fiber networks in the catalyst paper were subjected to methanol steam reforming (MSR) to produce hydrogen gas for fuel cell applications. They demonstrated a higher performance for methanol conversion and hydrogen production in the MSR reaction than commercial Cu/ZnO catalyst pellets, exhibiting an efficacy equivalent to that of the original catalyst powders. The surface properties of the ceramic fibers play a very important role in these applications. The surface of ceramic fibers can be modified by various techniques. Antimony-doped tin oxide coatings were deposited on the Nextel cloths by the sol-gel process.³ Diamond-coated ceramic fibers have been fabricated using hot filament CVD and tested for mechanical stiffness. Mechanical bend tests indicated that the fibers were significantly stiffened by the deposition of a CVD diamond layer of a few micrometers in thickness, giving a Young's modulus value close to that for natural diamonds.⁴

Physical vapor deposition (PVD) has also been increasingly used in surface modification in many industries. The wet bath technologies, such as the electroplating of finishes, have been recognized as a major source of environmental pollution. PVD coatings show the most promising solution for many industries.⁵ The most commonly used technique in PVD technology is sputter coating.⁶ Sputtering is using a mechanism with a sealing chamber, in which atoms or molecules are ejected from the surface of a target material as a result of collision with high-energy ions. These ejected atoms or molecules have certain kinetic energy and orientation that cause them to condense on the substrate and form a thin film.

Q. Wei (✉), D. Shao, B. Deng, Q. Xu
Key Laboratory of Eco-textiles, Ministry of Education,
Jiangnan University, Wuxi 214122, People's Republic of
China
e-mail: qfwei@jiangnan.edu.cn

The ability to deposit well-controlled coatings would expand the applications of ceramic fibers, based on changes to both their physical and chemical properties. In this study, ceramic fabrics were functionalized using metal sputter coatings. The surface morphology and properties of the materials were characterized by atomic force microscopy (AFM), environmental scanning electron microscopy (ESEM), and electrical resistance measurement. The interfacial adhesion between the coating layer and the substrate was also studied.

Experimental

Materials preparation

The substrates used in this study were ceramic fiber woven fabric (Nextel 312 AF-30) supplied by 3M. The details of the materials are listed in Table 1. Before the sputter coatings, the materials were washed with ethanol and distilled water. After washing, the materials were dried in an oven at 60°C.

Sputtering coating

A magnetron sputter coating system (JZCK-420B) was used to deposit a nanolayer on the materials. A high-purity copper (Cu) target (99.999%) was mounted on the cathode, and the ceramic fiber substrate was placed on the anode with a side facing the target. Argon (99.999%) was used as the bombardment gas. The sputtering pressure was set at 3 Pa. The direct current power used for Cu sputtering was set at 100 W. The sputtering was performed on one side of the substrate, and the coating thickness of the deposition layer was measured using a coating thickness detector (FTM-V) fixed in the sputtering chamber. The thickness was set at 20, 50, and 100 nm, respectively. The sample holder with a rotation speed of 100 rpm was introduced to improve the uniformity of the deposition on ceramic fibers.

Surface characterization

Atomic force microscopy

The surface morphology of the ceramic fibers was examined by AFM. A Benyuan CSPM 3300 AFM was

Table 1: Specification of the ceramic material

	Weight (g/m ²)	Available widths (m)	Thickness (mm)
Nextel 312 AF-30	586	0.91	0.74

employed to image the morphology of the fiber surfaces. Scanning was carried out in contact mode AFM,⁷ with a silicon cantilever. All images were obtained in ambient conditions.

Energy dispersive X-ray system

The Philips XL30 ESEM-FEG, equipped with a Phoenix energy dispersive X-ray (EDX) analysis system, was used to examine the chemical compositions of the sputter-coated fibers. EDX is available in all modes in the ESEM, and all elements down to boron can be detected, including the light elements such as carbon, nitrogen, and oxygen.⁸ In the EDX analysis, an accelerating voltage of 20 kV with accounting time of 100 s was applied.

Electrical resistance

The resistivity was measured by the four-point probe method (Baishen Technology, China). These four probes with $\Phi 0.5$ mm are all made by Tungsten Carbide, and the distance between each two probes is 1 mm. Samples were all tested three times in the same direction and then the average values were obtained.

Peel-off test

The peel-off test was performed on a Zwick universal materials testing machine to examine the interfacial adhesion of the coated layer. The test speed was set at 200 mm/min in this study. The initial distance was 10 mm. The tape used was 3M600 test adhesive tape. The test samples were cut into 7×2.5 cm² pieces for the peel-off test. The samples were pressed with a load of 400 g for 12 h before the peel-off test. The all tests were performed at $20 \pm 2^\circ\text{C}$ and $65 \pm 2\%$ relative humidity. Each test was carried out three times and the average values were reported.

Results and discussion

Surface morphology

The surface morphology of the ceramic fibers is presented in Fig. 1a. The AFM image shows the relatively smooth surface with clear groove-like structures on the fiber surface. These groove-like structures are formed during the processing of fibers. The sputter coating significantly alters the surface characteristics of the ceramic fibers, as indicated in Figs. 1b, 1c and 1d.

The AFM observations clearly reveal the change in surface morphology of the ceramic fibers sputter-coated with a copper layer. The sputtered copper layer covers up the original structures, and the deposited

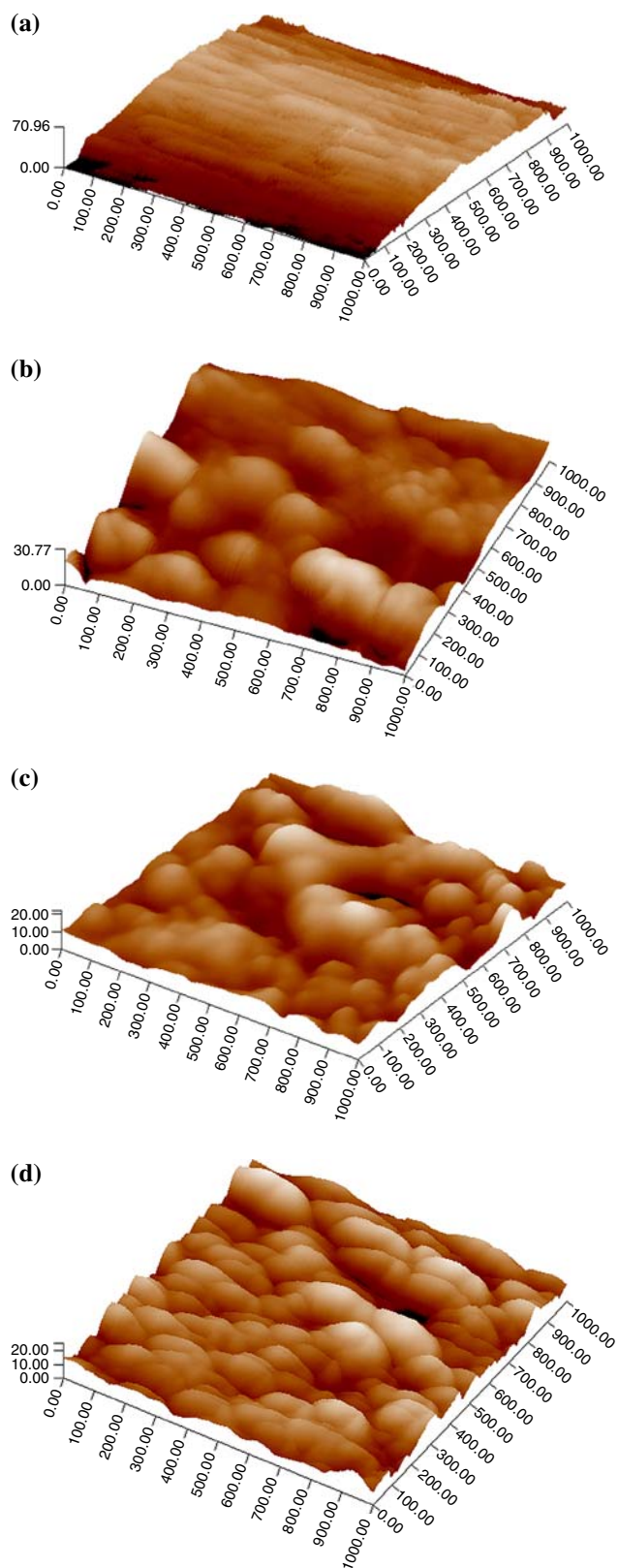


Fig. 1: Surface morphology of the ceramic fibers in AFM: (a) original fiber; (b) 20 nm Cu-coated fiber; (c) 50 nm Cu-coated fiber; and (d) 100 nm Cu-coated fiber

particles form porous structures on the fiber surface when the deposition is only 20 nm. The AFM image also reveals that the average size of the sputtered Cu clusters is about 17.5 nm. The deposition becomes much more compact, as presented in Fig. 1c, when the coating thickness is increased to 50 nm. This is attributed to the growth of the sputtered Cu grains during the coating process. The average size of the Cu nanocluster is also increased to 24.5 nm as the coating thickness is increased to 50 nm. Figure 1d shows the Cu coating of 100 nm in thickness. It is clear that the deposited particles are much denser compared to those shown in Figs. 1b and 1c. The average size of the Cu grain is increased to almost 36 nm. The growth of the sputtered Cu grains during the coating process leads to the formation of larger particles and better coverage of the copper layer on the ceramic fibers.

EDX analysis

The copper deposition on the ceramic fiber surface is also revealed by EDX analysis, as illustrated in Fig. 2. Figure 2a shows the EDX spectrum of the ceramic fibers without copper coating. The spectrum clearly reveals the main composition of aluminum (Al), silicon (Si), and oxygen (O) in the ceramic fibers.

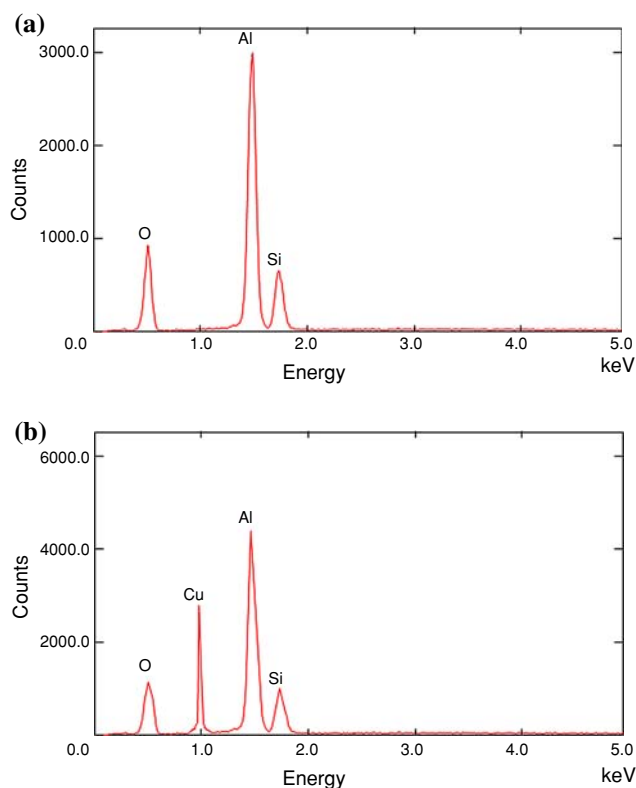
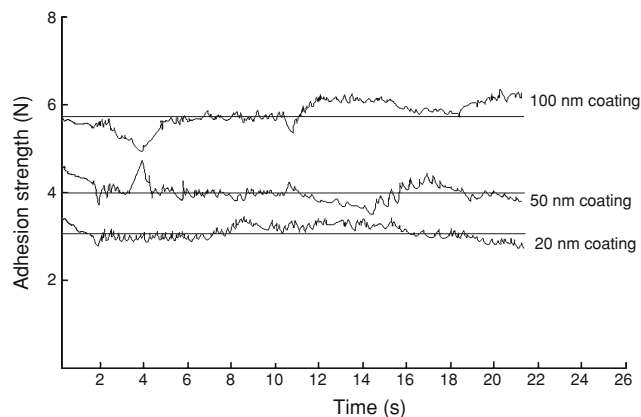


Fig. 2: EDX spectra of the samples: (a) original fibers and (b) 20 nm Cu-coated fiber

Table 2: Surface resistance

	Original	20 nm coating	50 nm coating	100 nm coating
Resistivity (Ω cm)	Out of range (over 10^6)	7568.2 ± 128.3	1496.5 ± 57.6	535.7 ± 15.2

**Fig. 3: Peel-off test of the samples**

A significant amount of copper (Cu) on the fiber surface after sputter coating can be seen in Fig. 2b, when the copper coating is only 20 nm. It is also observed that the increase in the coating thickness leads to an increase in the amount of Cu detected on the ceramic fibers. The EDX analysis confirms the formation of the copper deposition on the ceramic fibers.

Resistance analysis

The results of resistance measurements of the samples are listed in Table 2. The table clearly shows that the surface resistance of the ceramic fabric (Nextel 312-AF30) before the copper sputter coating is over $10^6 \Omega$ cm, indicating the electrical insulation behavior of the ceramic fabric.

The surface resistance of the fabric drops from over $10^6 \Omega$ cm to about 7568.2Ω cm when the coating thickness is only 20 nm. The measured surface resistance indicates the change in surface conductivity of the ceramic fabric. The 20 nm copper coating significantly changes the surface conductivity of the ceramic fabric. The increase in sputtering thickness can lower the surface resistance of the substrate, as presented in Table 2. It is clear that the surface resistance is further lowered to about 1496.5Ω cm when the copper coating reaches 50 nm. The growth of the sputtered Cu grains, and better coverage of the copper layer on the ceramic fibers, lead to the improvement in surface conductivity as the coating thickness increases. The surface resistance of the ceramic fabric is only 535.7Ω cm when the coating thickness is increased to 100 nm.

The table also reveals that the coating thickness has a certain effect on the deviation of surface

resistance of the materials. The increase in coating thickness leads to a decrease in the deviation of the surface resistance. This is also attributed to the growth of the sputtered Cu grains and better coverage of the copper layer on the ceramic fibers as the coating thickness is increased.

Coating adhesion

The adhesion between the sputtered nanoclusters and the ceramic fabric was examined by a peel-off test. The results of the peel-off test are presented in Fig. 3. It is shown that the average adhesion of the sputtered Cu nanoclusters to the ceramic fabric is about 3.2 N when the copper coating is 20 nm, as indicated in Fig. 3. The adhesion is increased to about 4.0 N when the coating thickness reaches 50 nm. The growth of the sputtered Cu grains and better coverage of the copper layer on the ceramic fabric contribute to the increase in the adhesion of the deposited copper layer to the ceramic fabric substrate. It is clearly shown in Fig. 3 that the adhesion is further increased to 5.6 N as the coating thickness is increased to 100 nm. The sputtered copper particles hit the fabric surface and knock off some previously deposited particles that have poor adhesion between the coating and the substrate. This effect will enhance the adhesion of the deposited particles to the fabric as the coating time increases.

Figure 3 also reveals the adhesion fluctuation during the peel-off test. This phenomenon is generated by the uneven surface of the woven structure of the ceramic fabric, in which the two systems of yarns (warp and weft) are interlaced to form a weave structure.⁹

Conclusion

This study has investigated the surface functionalization of ceramic fabric using a sputter coating of copper. The copper coating significantly altered the surface morphology of the ceramic fibers. The surface conductivity of the material was also significantly improved. The adhesion of the coating layer to the fabric was also investigated in this work. The surface functionalization of ceramic fabrics will improve the surface properties of the materials and expand the potential applications of these materials.

Acknowledgment This work was supported by the Program for New Century Excellent Talents in University (NCET-06-0485), and the Natural Science Foundation of Jiangsu Province (BK2008106).

References

1. Wilson, DM, Visser, LR, "High Performance Oxide Fibers for Metal and Ceramic Composites." *Compos. A: Appl. Sci. Manuf.*, **32** 1143–1150 (2001). doi:[10.1016/S1359-835X\(00\)00176-7](https://doi.org/10.1016/S1359-835X(00)00176-7)
2. Fukahori, S, Kitaoka, T, Tomoda, A, Suzuki, R, Wariishi, H, "Methanol Steam Reforming Over Paper-Like Composites of Cu/ZnO Catalyst and Ceramic Fiber." *Appl. Catal. A: Gen.*, **300** 155–161 (2006). doi:[10.1016/j.apcata.2005.11.008](https://doi.org/10.1016/j.apcata.2005.11.008)
3. Park, SS, Zheng, HX, Mackenzie, JD, "Sol-Gel Derived Antimony-Doped Tin Oxide Coatings on Ceramic Cloths." *Mater. Lett.*, **22** 175–180 (1995). doi:[10.1016/0167-577X\(94\)00241-X](https://doi.org/10.1016/0167-577X(94)00241-X)
4. May, PW, Rego, CA, Ashfold, MNR, Rosser, KN, Lu, G, Walsh, TD, Holt, L, Everitt, NM, Partridge, PG, "CVD Diamond-Coated Fibres." *Diamond Relat. Mater.*, **4** 794–797 (1995). doi:[10.1016/0925-9635\(94\)05279-4](https://doi.org/10.1016/0925-9635(94)05279-4)
5. Navinšek, B, Panjan, P, Milošev, I, "PVD Coatings as an Environmentally Clean Alternative to Electroplating and Electroless Processes." *Surf. Coat. Technol.*, **116–119** 476–487 (1999). doi:[10.1016/S0257-8972\(99\)00145-0](https://doi.org/10.1016/S0257-8972(99)00145-0)
6. Atkinson, A, Moseley, PT, "Thin Film Electroceramics." *Appl. Surf. Sci.*, **65–66** 212–2192 (1993). doi:[10.1016/0169-4332\(93\)90661-T](https://doi.org/10.1016/0169-4332(93)90661-T)
7. Baklanova, NI, Zaitsev, BN, Titov, AT, Zima, TM, "The Chemistry, Morphology, Topography of Titanium Carbide Modified Carbon Fibers." *Carbon*, **46** 261–271 (2008). doi:[10.1016/j.carbon.2007.11.019](https://doi.org/10.1016/j.carbon.2007.11.019)
8. Leemann, A, Holzer, L, "Alkali-Aggregate Reaction—Identifying Reactive Silicates in Complex Aggregates by ESEM Observation of Dissolution Features." *Cem. Concr. Compos.*, **27** 796–801 (2005). doi:[10.1016/j.cemconcomp.2005.03.007](https://doi.org/10.1016/j.cemconcomp.2005.03.007)
9. Szosland, J, "Modeling the Structural Barrier Ability of Woven Fabrics." *AUTEX Res. J.*, **3** 102–109 (2003)